Journal of Controlled Release 164 (2012) 283–290

Contents lists available at SciVerse ScienceDirect

Journal of Controlled Release

journal homepage: www.elsevier.com/locate/jconrel

Differential loading methods for BMP-2 within injectable calcium phosphate cement

Floor C.J. van de Watering [a], Janneke D.M. Molkenboer-Kuenen [b], Otto C. Boerman [b], Jeroen J.J.P. van den Beucken [a], John A. Jansen [a,*]

[a] Department of Biomaterials, Radboud University Nijmegen Medical Center, PO Box 9101, 6500 HB Nijmegen, The Netherlands
[b] Department of Nuclear Medicine, Radboud University Nijmegen Medical Centre, PO Box 9101, 6500 HB, Nijmegen, The Netherlands

ARTICLE INFO

Article history:
Received 27 March 2012
Accepted 8 July 2012
Available online 16 July 2012

Keywords:
Calcium phosphate cement
Growth factor release
rhBMP-2
In vivo response

ABSTRACT

Clinical application of calcium phosphate cement (CPC; with incorporated polymeric porogens) in an injectable form implicates that loading methods for growth factors are limited. In view of this, the current study evaluated the in vitro and in vivo release kinetics of bone morphogenetic protein-2 (BMP-2) loaded on poly(D,L-lactic-co-glycolic acid) (PLGA) microparticles (CPC/PLGA), BMP-2 incorporation into the liquid phase of CPC (CPC/liquid), and BMP-2 absorbed to the surface of preset, porous CPC (CPC/surface) as a control via an in vitro release experiment and in vivo using microSPECT imaging with ^{125}I-labeled BMP-2. In addition, the osteoinductive capacity of scaffolds generated via the different BMP-2 loading methods was assessed in a subcutaneous rat model. Additional controls consisted of porous CPC scaffolds (CPC/porous) and CPC/PLGA (CPC/control) without BMP-2 loading. The results revealed that it is feasible to load BMP-2 into CPC via adsorption to PLGA-microparticles or the liquid phase of CPC, which resulted in a similar release profile over the course of 28 days, despite distinct protein distribution patterns. Compared to CPC-scaffolds with surface-loaded BMP-2, these loading methods showed a similar release profile, except for a significantly decreased burst release. As such, the observed osteoinductive capacity for only CPC-scaffolds with surface-loaded BMP-2 is likely to be related to this difference in burst release. It remains unclear to what extent the differential BMP-2 loading methods for injectable CPC can affect the biological response in a bone environment.
© 2012 Elsevier B.V. All rights reserved.

1. Introduction

Calcium phosphate (CaP) based materials are widely used as bone substitute materials in orthopedic, reconstructive and oral surgery due to their performance [1,2]. CaP-based materials are available in various forms, for example as granules or blocks. More interestingly, injectable CaP-based pastes (e.g. of brushite or apatitic nature [3]) are also available and have the advantage of optimal bone defect filling through minimally invasive surgery. Injectable CaP-based cements have shown biocompatibility and osteoconductivity, although in vivo degradation and tissue ingrowth were difficult to control [1,4,5].

To enhance material degradation, different approaches have been explored to introduce porosity within CaP cement (CPC), including the use of sodium bicarbonate to obtain CO_2-gas bubbles during cement setting and mixing biodegradable polymer microparticles (e.g. gelatin [6] or poly(D,L-lactic-co-glycolic acid) (PLGA) [7–10]) as porogens homogeneously through the cement powder. Although porosity is instantaneous when using the CO_2-gas bubble method, the lack of control on pore size and distribution is disadvantageous [11]. In contrast, PLGA-microparticles create a delayed porosity, after the PLGA-microparticles are degraded by means of hydrolysis in a process called bulk erosion [10], with, importantly, homogeneously dispersed pores of desired size. In addition, Félix Lanao, Leeuwenburgh, Wolke, and Jansen [12] reported that the hydrolysis of PLGA-microparticles can be controlled depending on the PLGA molecular weight, end-group chemistry, and/or morphology. In view of this, CPC degradation and bone formation were shown to be highest when dense acid-terminated PLGA-microparticles were incorporated in CPC [13].

Further empowerment of CPC for biological performance can be achieved by incorporating biologically active compounds, including growth factors. Previously, it has been reported that biologically active additives can be absorbed on preset CPC. For example, CPC surface loading of the growth factor bone morphogenetic protein-2 (BMP-2) demonstrated to induce bone formation at ectopic locations in rats [14] and rabbits [15] and increased bone formation at orthotopic locations in rabbits [16]. However, the clinical application of CPC is in an injectable form, for which the loading of additives on the surface of preset CPC is not feasible. Consequently, a biologically active compound needs to be incorporated during the CPC setting (i.e. included into the powder or the liquid phase of CPC). In view of this, growth factor loading onto included porogens (e.g. PLGA-microparticles) represents an approach to introduce biologically active compounds for the injectable CPC. It has been reported that incorporation of BMP-2 adsorbed PLGA-microparticles

* Corresponding author at: Department of Biomaterials (309), Radboud University Nijmegen Medical Center, PO Box 9101, 6500 HB Nijmegen, The Netherlands. Tel.: +31 24 3614006; fax: +31 24 361 4657.
E-mail address: J.Jansen@dent.umcn.nl (J.A. Jansen).
URL: http://www.biomaterials-umcn.nl (J.A. Jansen).

0168-3659/$ – see front matter © 2012 Elsevier B.V. All rights reserved.
doi:10.1016/j.jconrel.2012.07.007

Table 1
Overview of the different compositions.

Group	CPC (wt.%)	PLGA (wt.%) Hollow or Dense	PLGA burnt out	BMP-2 added to
CPC/porous	70	30 (H)	Yes	–
CPC/control	70	30 (D)	No	–
CPC/PLGA	70	30 (D)	No	PLGA-porogens
CPC/liquid	70	30 (D)	No	Liquid phase
CPC/surface	70	30 (H)	Yes	Surface

into CPC results in a sustained in vivo release of the growth factor at both ectopic [17] and orthotopic locations [18] in rats, and an increased bone formation was observed compared to non-loaded scaffolds at orthotopic locations [18]. Another approach is to add biologically active compounds to the liquid phase of CPC. It has been reported that the inclusion of transforming growth factor (TGF)-β1 to the liquid phase of CPC increased the formation of bone in rat calvarial bone defects [19]. Since growth factor release and related biological effect are likely to be carrier dependent, the release kinetics and osteoinductive capacity of different loading approaches need to be evaluated.

In the present study, different loading methods for BMP-2 into CPC were evaluated in terms of in vitro and in vivo release and in vivo osteoinductive capacity. For injectable CPC, BMP-2 was either adsorbed onto dense PLGA-microparticles or added to the liquid phase of CPC. For comparison, BMP-2 was loaded onto the surface of pre-set, porous CPC. Radiolabeled BMP-2 was used to monitor release profiles in vitro as well as in vivo using a subcutaneous rat model, in which growth factor retention was analyzed via single-photon emission computed tomography (SPECT). BMP-2 loaded scaffolds without radiolabel were histologically analyzed for osteoinductive capacity of the different loading methods in a rat subcutaneous implantation model. It was hypothesized that in view of an injectable CPC, the addition of BMP-2 via incorporated PLGA-microparticles would result in an increased BMP-2 release and subsequent improved osteoinductive properties in CPC/PLGA compared to CPC/liquid due to a faster degradation of the PLGA-microparticles compared to that of the ceramic matrix of CPC.

2. Materials and methods

2.1. Materials

Calcium phosphate cement (CPC) consisted of 85% alpha tri-calcium phosphate (α-TCP; CAM Bioceramics BV, Leiden, The Netherlands), 10% dicalcium phosphate anhydrous (DCPA; J.T. Baker Chemical Co., USA) and 5% precipitated hydroxyapatite (pHA; Merck, Darmstadt, Germany), and was sterilized using gamma irradiation (>25 kGy; Isotron BV, Ede, The Netherlands). The cement liquid applied was a sterilized 2 wt.% aqueous solution of Na_2HPO_4. Acid terminated poly(D,L-lactic-co-glycolic acid) (PLGA; Purasorb®, Purac Biomaterials BV, Gorinchem, The Netherlands) with a lactic to glycolic acid ratio of 50:50 and a molecular weight (Mw) of 17 ± 0.02 kg/mol was used for microparticle preparation. Commercially available recombinant human BMP-2 (BMP-2; R&D Systems MN, USA) was used.

2.2. Methods

2.2.1. Analysis of the BMP-2 secondary structure

Circular dichroism (CD) spectra of BMP-2 (0.1 mg/mL) dissolved in 2 wt.% aqueous solution of Na_2HPO_4 or BMP-2 (0.1 mg/mL) dissolved in PBS were recorded in the range 195–260 nm at a scan rate of 2 s per nm with a Jasco J-810 spectropolarimeter (Oklahoma City, OK) to visualize protein conformation. A quartz cell of 0.1 cm thickness was used. CD spectra values were expressed as mean residue ellipticities (in degrees cm^{-2} $dmol^{-1}$). The results were further subjected to a non-linear regression analysis to illustrate the secondary structure using the Gauss–Newton algorithm method.

Table 2
Secondary structure analysis of BMP-2 dissolved in 2% Na_2HPO_4 or PBS.

	α-Helix	β-Sheet	Random coil (%)
BMP-2 dissolved in PBS	14	40	40
BMP-2 dissolved in 2% Na_2HPO_4	14	40	40

The analysis was conducted based on the CD spectrum using the Gauss-Newton algorithm method.

2.2.2. Preparation of hollow and dense PLGA-microparticles

To prepare hollow PLGA-microparticles of around 50 μm in diameter, a double-emulsion-solvent-extraction technique (water-in-oil-in-water) was used, as described previously [10]. Microparticles were produced by adding 500 μl of distilled water to 1400 mg PLGA in 2 mL dichloromethane (DCM). The mixture was emulsified using a Turrax® emulsifier for 60 s at 6000 rpm. Then, 6 mL 0.3% aqueous poly(vinyl alcohol) (PVA, Acros Organics, Geel, Belgium) solution was added and emulsified for another 60 s at 6000 rpm to produce the second emulsion. The emulsion was transferred to a stirred beaker, after which 394 mL 0.3% PVA solution and 400 mL of 2% isopropylic alcohol solution were added slowly. After 1 h of stirring, the microparticles were allowed to settle for 15 min and the solution was decanted. Then, the microparticles were washed and collected through centrifugation at 1500 rpm for 5 min, lyophilized and stored at −20 °C until use. The size distribution of the microparticles was determined by image analysis (Leica Qwin®, Leica Microsystems). The microparticles were imaged by scanning electron microscopy (SEM; JEOL6310 at 15 kV).

To prepare dense PLGA-microparticles of around 50 μm in diameter, a single-emulsion technique was used, as described before [12]. Microparticles were produced by dissolving 0.4 g of PLGA in 4 mL DCM. The solution was transferred into a stirred beaker containing 150 mL of 0.3% PVA solution and 50 mL of 2% IPN solution. After 1 h of stirring, the microparticles were allowed to settle for 1 h min and the solution was decanted. Then, the microparticles were washed and collected through centrifugation at 1500 rpm for 1 min and lyophilized. Subsequently, the microparticles were sterilized by gamma irradiation (>25 kGy; Isotron BV, Ede, The Netherlands) and stored at −20 °C until use. The size distribution of the microparticles was determined by image analysis (Leica Qwin®, Leica Microsystems). The microparticles were imaged by scanning electron microscopy (SEM; JEOL6310 at 15 kV).

2.2.3. ^{125}I-labeling of BMP-2

BMP-2 was labeled with ^{125}I, as described previously [20]. Briefly, in a 500 μl eppendorf tube coated with 100 μg iodogen, 10 μl of 0.5 M phosphate buffer saline (PBS) was added. Growth factor (75 μg) and 3 mCi ^{125}I (Perkin-Elmer, Boston, MA) was added and incubated at room temperature for 10 min. To remove the non-incorporated ^{125}I, the reaction mixture was loaded onto a pre-rinsed disposable Sephadex G-25 column (NAP5; GE healthcare Bio-Sciences AB, Uppsala, Sweden) that was eluted with PBS, 0.1% BSA. The labeling efficiency of the procedure was 55% and the specific activity of the labeled protein was 22.0 μCi/μg.

2.2.4. Experimental groups

The following experimental groups were generated (for composition see Table 1):

1. CPC/control (pre-set dense CPC scaffold containing dense PLGA-microparticles)
2. CPC/porous (pre-set instant porous CPC scaffold; PLGA-microparticles burnt out)
3. CPC/PLGA (CPC/control scaffold with BMP-2 adsorbed onto dense PLGA-microparticles)
4. CPC/liquid (CPC/control scaffold with BMP-2 added to the liquid phase)
5. CPC/surface (CPC/porous scaffold with BMP-2 loaded on the surface)

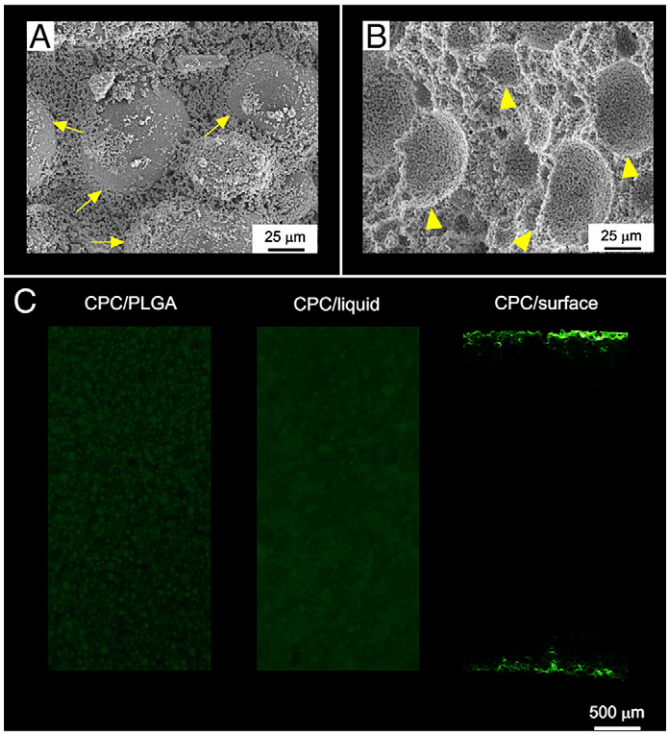

Fig. 1. Characterization of scaffold material. Microscopic SEM images of scaffold material (A) CPC/control and (B) CPC/porous. Original magnification is 75×, bar represents 25 μm. PLGA-microparticles (arrows) and created pores after burning out PLGA-microparticles (arrowheads) are indicated. (C) Protein distribution using alexa fluor 488 labeled BSA as a model protein. BSA was loaded on PLGA-microparticles and incorporated in CPC (CPC/PLGA), included in liquid phase of CPC (CPC/liquid) or absorbed onto the surface of instantly porous preset CPC (CPC/surface). Bar represents 500 μm.

2.2.5. Preparation of CPC/PLGA scaffolds

For the in vitro release experiment, the scaffolds were loaded with ^{125}I-BMP-2 solutions using a hot/cold mixture of BMP-2, containing 0.5 μCi per scaffold. For the in vivo release experiment, the scaffolds were loaded with ^{125}I-BMP-2 solutions using a hot/cold mixture of BMP-2, containing 15 μCi per scaffold. For the evaluation of the osteoinductive capacity of the different loading methods, BMP-2 without radiolabel was used.

The different experimental groups were generated as previously reported (for CPC/porous and CPC/surface see [14]; for CPC/control, CPC/PLGA and CPC/liquid see [12]; for composition see Table 1). In short, 0.69 g dense or 0.3 g hollow PLGA-microparticles were added to 0.7 g sterile CPC, after which sterile Na_2HPO_4 solution was added to the CPC/PLGA in a liquid/powder ratio of 0.40 and mixed for 20 s. After mixing, the cement was immediately injected into a Teflon mold to ensure a standardized shape of the scaffolds (Ø 7.8 mm, height 2.8 mm). For CPC/porous and CPC/surface, an instantaneous open porous structure was created by placing the pre-set scaffolds in a furnace at 650 °C for 2 h to burn out the polymer.

For the adsorption of BMP-2 to the PLGA-particles, a volume of 240 μl 0.1% BSA/PBS solution containing 10 μg BMP-2 was added to the sterile dense PLGA-microparticles, after which the microparticles were frozen, lyophilized and used. To include BMP-2 in the liquid phase of CPC, a Na_2HPO_4 solution containing 10 μg BMP-2 was used. For surface-loaded BMP-2, a volume of 30 μl growth factor solution containing 5 μg BMP-2 was applied to the surface of each side of the instantaneous open porous scaffold to obtain 10 μg BMP-2/scaffold. Thereafter, the scaffolds were frozen and lyophilized.

2.2.6. Characterization of scaffold material

2.2.6.1. Porosity measurements. To determine total porosity of the scaffolds, CPC/control and CPC/porous ($n=6$) were placed in a furnace at 650 °C for 2 h to burn out the polymer. Subsequently, the microporosity and total porosity were calculated using the following equations [10]:

$$_{\varepsilon}\varepsilon_{tot} = \left(1 - \frac{\text{mburnt}}{V * \rho HAP}\right) * 100\% \quad (1)$$

$$\varepsilon_{micro} = \left(1 - \frac{\text{mburnt}}{\text{mnanoporous}}\right) * 100\% \quad (2)$$

Legend

ε_{tot}	total porosity (%)
ε_{micro}	microporosity (%)
m_{burnt}	average mass sample (after burning out polymer) (g)
$m_{nanoporous}$	average mass intrinsic nanoporous sample (g)
V	volume sample (cm^3)
ρ_{HAP}	density hydroxyl apatite (g/cm^3)

2.2.6.2. Scanning electron microscopy (SEM). CPC/control and CPC/porous scaffolds were sputter-coated with gold and examined and photographed using SEM (Jeol 6310, Nieuw-Vennep, The Netherlands) at an acceleration voltage of 10 kV.

2.2.6.3. Distribution of protein in the different formulations. To visualize the distribution of added protein when adsorbed or included in the different scaffolds, albumin from bovine serum (BSA) labeled with Alexa Fluor 488 (Invitrogen, Life Technologies Europe BV, Bleiswijk, The Netherlands) was used as a model protein. The loading of labeled BSA (10 μg BSA/scaffold) to the different CPCs was similar as described previously, resulting in groups 3, 4 and 5. The scaffolds were frozen, lyophilized and fixed in 4% formalin overnight. Subsequently, the tissue blocks were embedded

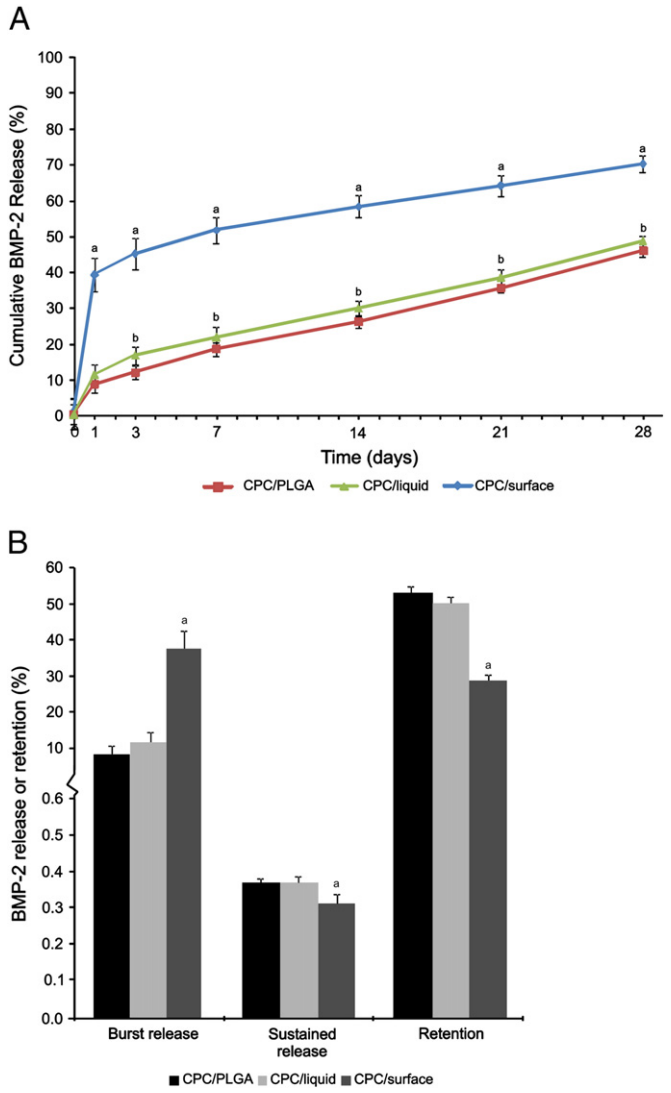

Fig. 2. Longitudinal in vitro scintigraphic assessment (A) CPC/PLGA, CPC/liquid and CPC/surface during 28 days and (B) the in vitro burst release (after 1 day), sustained release (the release per day from day 1–28) and the retention after 28 days. The release and retention is expressed as percentage of the ratio of initial loading amount. Bars represent the mean ± SD ($n = 6$). (a) $p < 0.001$ compared to CPC/PLGA and CPC/liquid, (b) $p < 0.01$ compared to CPC/PLGA.

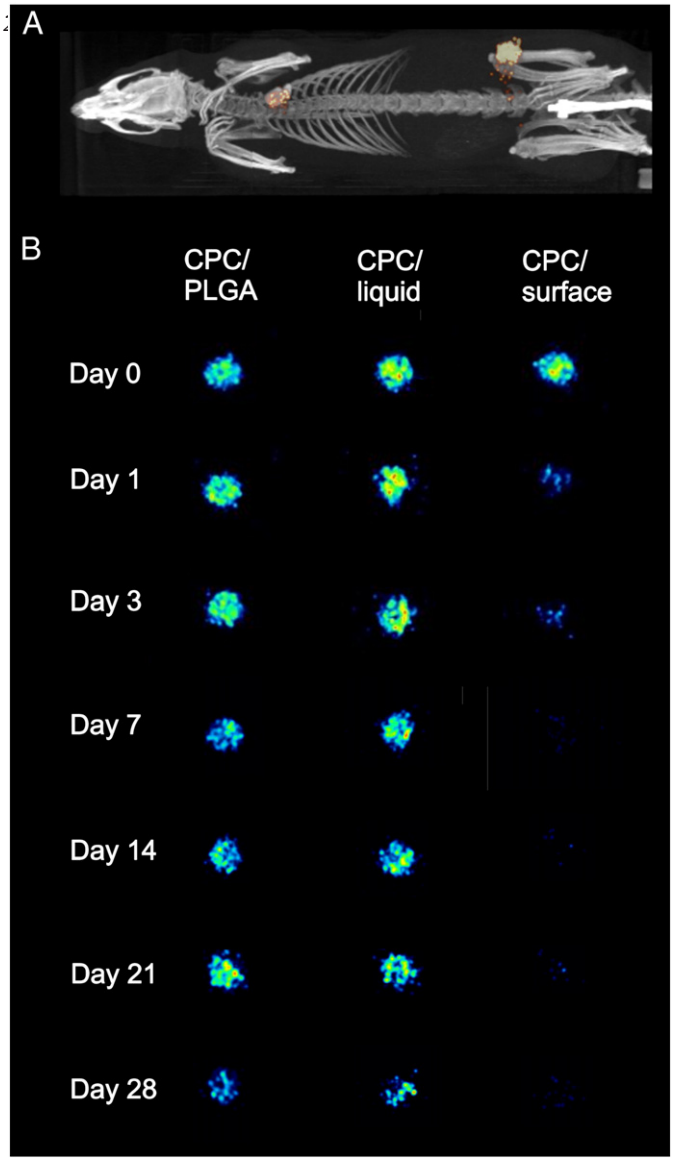

Fig. 3. (A) Representative U-SPECT/CT-scan of rat implanted with CPC scaffolds. (B) Representative U-SPECT scans of CPC/PLGA, CPC/liquid or CPC/surface during 28 days.

in methylmethacrylate (MMA). Perpendicular to the scaffold diameter, thin sections (~10 μm) were prepared using a microtome with diamond blade (Leica Microsystems SP 1600, Nussloch, Germany) [21]. The MMA sections were visualized using a fluorescence microscope with a Zeiss filter set 00, consisting of a 530–585 nm band-pass excitation filter (Carl Zeiss B.V., Sliedrecht, The Netherlands).

Table 3
Overview of implants placed, retrieved and used for histomorphometrical evaluation.

	Implants placed	Implants retrieved	Implants used for analysis
CPC/porous	3	3	3
CPC/control	3	3	3
CPC/PLGA	6	6	5[a]
CPC/liquid	6	6	5[a]
CPC/surface	6	6	5[a]

[a] Deviations from the number of implants retrieved due to fracturing of implants during histological processing.

The different CPC scaffolds loaded with ^{125}I-BMP-2 ($n = 6$; 0.5 μCi/scaffold) were placed in 10 mL glass vials for evaluation of the in vitro BMP-2 release kinetics and incubated in 3 mL PBS at 37 °C for 28 days. At days 1, 3, 7, 14, 21 and 28, the samples were carefully transferred to new vials containing fresh PBS, after which gamma emission of the scaffolds was measured in a shielded well-type gamma counter (Wizard, Pharmacia-LKB, Uppsala, Sweden). Standards were measured simultaneously to correct for radioactive decay. The remaining activity in the scaffolds was expressed as percentage of the initial dose.

2.2.8. In vivo experiment

2.2.8.1. Animals. Fifteen healthy young adult (8 weeks old) male Wistar rats were used as experimental animals, of which 9 animals were used for the in vivo release experiment (two implants per animal) and 6 animals were used to evaluate the osteoinductive capacity of the different CPC formulations (4 implants per animal). The research was reviewed and approved by the Experimental Animal Committee of the Radboud University (RUDEC 2011-186) and national guidelines for the care and use of laboratory animals were observed.

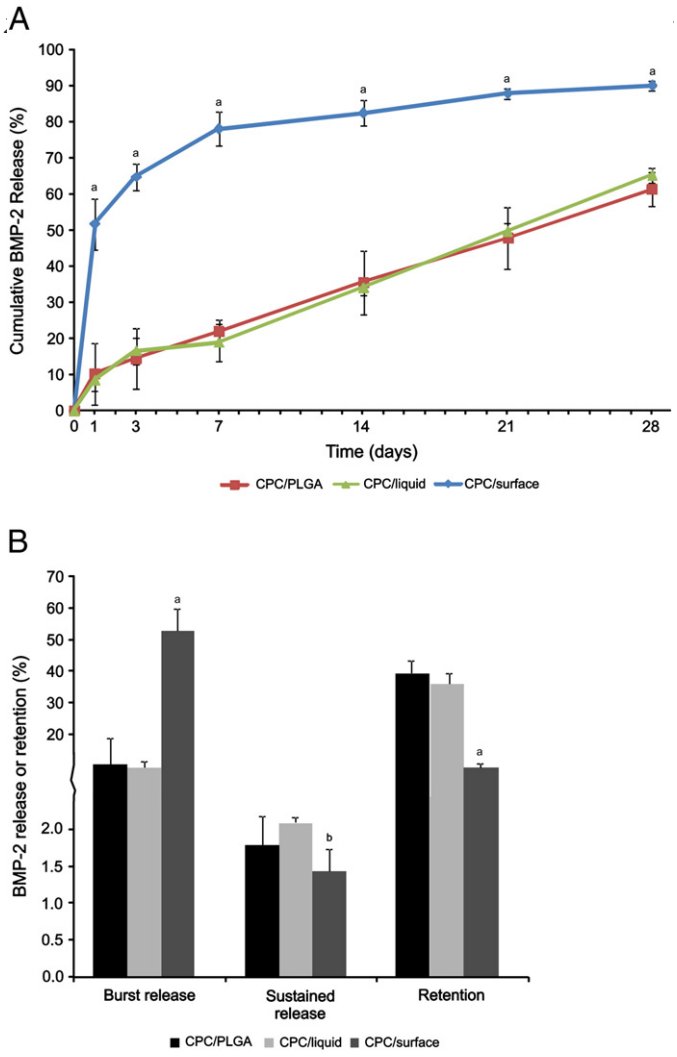

Fig. 4. Longitudinal in vivo (A) release assessment analyzed via a small animal U-SPECT II scanner of CPC/PLGA, CPC/liquid and CPC/surface during 28 days and (B) the in vitro burst release (after 1 day), sustained release (the release per day from day 1–28) and the retention after 28 days. The release and retention is expressed as percentage of the ratio of initial loading amount. Bars represent the mean ± SD ($n=4$). (a) $p<0.01$ compared to CPC/PLGA and CPC/liquid; (b) $p<0.05$ compared to CPC/liquid.

Isoflurane inhalation (Rhodia Organique Fine Limited, Avonmouth, Bristol, UK). To minimize post-operative discomfort, Rimadyl (Carprofen, Pfizer Animal Health, New York, USA) was administered subcutaneously (5 mg/kg) before the surgery. CPC scaffolds were subcutaneously implanted into the back of each rat. To insert the scaffolds, rats were immobilized on their abdomen and the skin was shaved and disinfected with chlorhexidine. On both sides of the vertebral column, two small paravertebral incisions were made through the full thickness of the skin. Lateral to the incisions, a subcutaneous pocket was created using blunt dissection. Subsequently, one implant was inserted into each pocket. Finally, the skin was closed using staples (Agraven, Instruvet, Boxmeer, The Netherlands). In total, for the in vivo release experiment eighteen implants (two implants per animal; $n=6$ for each experimental group) and for the osteoinductive capacity evaluation twenty-four implants (4 implants per animal; $n=3$ for groups 1–2 and $n=6$ for groups 3–5) were placed according to a randomization scheme.

The animals were housed in pairs. In the initial postoperative period, the intake of water and food was monitored. Further, the animals were observed for signs of pain, infection and proper activity. At the end of the implantation time, the rats were sacrificed by CO_2-suffocation.

2.2.8.3. In vivo release experiment. At days 0, 1, 3, 7, 14 and 21 after implantation of the CPC scaffolds, rats were scanned using a small-animal SPECT scanner (U-SPECT II, MILabs, The Netherlands). Anesthesia was induced and maintained by Isoflurane inhalation (Rhodia Organique Fine Limited, Avonmouth, Bristol, UK). On day 28, rats were sacrificed and scanned post mortem followed by a CT scan for anatomic reference. The animals were placed prone in the SPECT scanner and scanned for 40 min using a rat 1.0-mm-diameter-pinhole collimator tube. Scans were reconstructed with MILabs reconstruction software, which uses an ordered-subset expectation maximization algorithm, with a voxel size of 0.375 mm. The amount of radioactivity in a specified volume of interest around the implants was quantified and expressed as percentage of original dose per scaffold (PMOD software, version 3.15, PMOD Technologies Ltd.). To achieve accurate quantification, standards containing 0, 1, 3, 10 or 30 μCi ^{125}I were scanned at the same days.

2.2.8.4. Implant retrieval and histological preparations. The specimens without radiolabeled BMP-2 ($n=6$) were retrieved after a 4-week implantation period. After sacrifice, scaffolds with surrounding tissues were excised and fixed in 10% phosphate-buffered formaldehyde solution (pH 7.4). Subsequently, the tissue blocks were dehydrated in increasing ethanol concentrations (70–100%) and embedded in methylmethacrylate (MMA). Perpendicular to the diameter of the scaffolds, thin sections (10 μm) were prepared using a microtome with diamond blade (Leica Microsystems SP 1600, Nussloch, Germany) [21]. Three sections of each scaffold were stained with methylene blue and basic fuchsin and examined using light microscopy (Leica Microsystems AG, Wetzlar, Germany).

For CPC/PLGA, CPC/liquid and CPC/surface, two MMA samples were polished and gold sputter-coated prior to analysis with scanning electron microscopy (JEOL 6330) using Back-Scattered Electron (BSE) mode for histomorphometrical analysis.

2.2.8.5. Histological and histomorphometrical evaluation. Sections of MMA-embedded specimens (at least 3 sections per specimen) were quantitatively assessed using computer-based image analysis techniques (Leica® Qwin Pro-image analysis system, Wetzlar, Germany). The analysis technique is based on color recognition depending on staining intensity. From digital images (magnification: 5×), the total amount of newly-formed bone surrounding the CPC scaffold was determined and expressed in area measures (mm^2).

2.2.9. Statistical analysis

Statistical analysis was performed using GraphPad Instat 3.05 software (GraphPad Software Inc., San Diego, CA) using one-way analysis of variance with a Tukey multiple comparison post test. Differences were considered significant at p-values less than 0.05.

3. Results

3.1. Analysis of the BMP-2 secondary structure

CD spectra of BMP-2 dissolved in PBS or 2% Na_2HPO_4 were comparatively analyzed, showing only limited differences in molar CD values at 200–235 nm. Additionally, secondary structure analysis based on the obtained CD spectra revealed no significant differences in α-helix, β-sheet or random coil structure of BMP-2 dissolved in 2% Na_2HPO_4 compared to BMP-2 dissolved in PBS (Table 2).

3.2. Characterization of scaffold material

The preparation of hollow PLGA-microparticles with a double-emulsion-solvent-extraction technique and dense PLGA-microparticles with a single-emulsion technique resulted in microparticles with a similar average size of 58.4 ± 35.0 μm and 62.4 ± 28.9 μm ($p>0.05$), respectively.

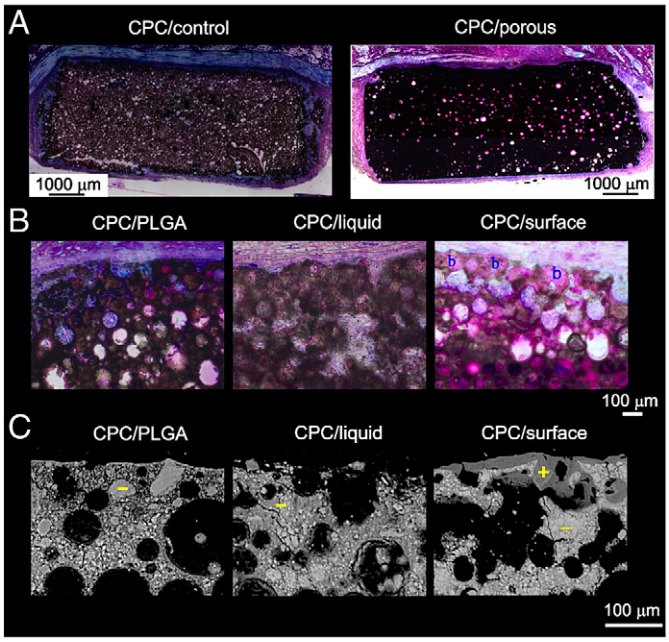

Fig. 5. (A) Histological overview sections of CPC/control and CPC/porous. Bar represents 1000 μm. Histological sections are stained with methylene blue and basic fuchsin. (B) Magnification of histological sections of CPC/PLGA, CPC/liquid and CPC/surface. Bone (b) is indicated in the sections. Original magnification is 20×. Bar represents 100 μm. Histological sections are stained with methylene blue and basic fuchsin. (C) Cross-sections observed with back scattering SEM of CPC/PLGA, CPC/liquid and CPC/surface. For back scattering SEM micrographs bone appears dark gray (+) while the CPC scaffold is lighter (−).

Since the principle of CPC preparation was based on either combination of CPC with hollow PLGA-microparticles (CPC/porous and CPC/surface) or CPC with dense PLGA-microparticles (CPC/control, CPC/PLGA and CPC/liquid), surface examination of the scaffolds was carried out for only CPC/porous and CPC/control. Surface examination showed that for CPC/control, a homogenous distribution of PLGA-microparticles within the implant material was observed (Fig. 1A). For CPC/porous, PLGA-microparticles were completely burnt out and an instant porous scaffold material was observed (Fig. 1B). Porosity measurements of CPC/porous and CPC/control scaffolds demonstrated a microporosity of 42.5 ± 3.0% and 59.9 ± 2.9% and a total porosity of 72.3 ± 1.4% and 80.7 ± 1.4% for CPC/porous and CPC/control, respectively.

Protein distribution was visualized using Alexa Fluor 488-labeled BSA as a model protein (Fig. 1C). The protein in CPC/surface was only observed peripherally and not in the center of the implants. In contrast, the protein in CPC/PLGA and CPC/liquid was distributed throughout the entire scaffold, showing localization of protein on the PLGA-microparticles for CPC/PLGA and a more dispersed pattern for CPC/liquid.

3.3. In vitro release

The in vitro release for CPC/PLGA, CPC/liquid and CPC/surface, during 28 days is depicted in Fig. 2. All scaffolds retained their integrity during the entire experiment. CPC/surface showed an initial burst release within 1 day (~40%), followed by a sustained release till day 28 (Fig. 2A). Both CPC/PLGA and CPC/liquid showed a limited burst release within 1 day (~10%), followed by a sustained release from day 1 till day 28 with a similar pattern compared to CPC/surface (Fig. 2A).

The cumulative BMP-2 release was significantly higher for CPC/surface compared to CPC/PLGA and CPC/liquid, reaching after 28 days a release of 70.0 ± 2.2%, 45.7 ± 1.7% and 48.4 ± 1.5%, respectively ($p<0.0001$; Fig. 2A). From day 3 onward, the cumulative BMP-2 release from CPC/liquid was significantly higher compared to CPC/PLGA ($p<0.01$; Fig. 2A).

The relative amounts of BMP-2 released during the different phases (i.e. burst release, sustained release, and retained BMP-2 after 28 days) are depicted in Fig. 2B. For CPC/surface, the burst release was significantly higher compared to CPC/PLGA and CPC/liquid (Fig. 2B; $p<0.001$; for CPC/PLGA 10.5 ± 2.3% and for CPC/liquid 13.1 ± 2.7%; for CPC/surface 40.4 ± 4.6%). The release rate per day from day 1–28 (Fig. 2B) of CPC/surface compared to CPC/PLGA and CPC/liquid was significantly lower ($p<0.0001$, release rate of 0.53 ± 0.02%, 0.52 ± 0.02% and 0.40 ± 0.03% per day for CPC/PLGA and CPC/liquid, CPC/surface, respectively). After 28 days, the retention for CPC/surface was significantly lower compared to CPC/PLGA and CPC/liquid ($p<0.0001$, retention of 54.3 ± 1.7%, 51.6 ± 1.5% and 30.0 ± 2.2% for CPC/PLGA, CPC/liquid and CPC/surface, respectively).

3.4. In vivo experiment

3.4.1. General observation of the experimental animals

All 6 animals used for the evaluation of the osteoinductive capacity of the different formulations, recovered uneventfully from the surgical procedure and remained in good health. From the 9 animals used for the in vivo release experiment, one animal died after 21 days. Clinical examination indicated that the cause of death was an anesthetic-induced respiratory depression during in vivo scanning. All remaining 8 animals recovered uneventfully from the surgical procedure and remained in good health. The total number of implants placed, retrieved and used for histomorphometrical evaluation is depicted in Table 3.

3.4.2. In vivo release

The in vivo release during 28 days from CPC/PLGA, CPC/liquid and CPC/surface, is depicted in Fig. 3. CPC/surface showed an initial burst release within 1 day followed by a sustained release from day 1 till day 28 (Fig. 4A). Both CPC/PLGA and CPC/liquid showed a limited burst release within 1 day (~10%), followed by a sustained release from day 1 till day 28 with a similar pattern compared to CPC/surface (Fig. 4A). The cumulative BMP-2 release was significantly higher for CPC/surface compared to CPC/PLGA and CPC/liquid reaching up to 90.1 ± 1.3%, 61.3 ± 4.7 and 65.2 ± 1.9% after 28 days, respectively ($p<0.0001$; Fig. 4A).

The relative amounts of BMP-2 released during the different phases (i.e. burst release, sustained release, and retained BMP-2 after 28 days) are depicted in Fig. 4B. For CPC/surface, the burst release was significantly higher

compared to CPC/PLGA and CPC/liquid (Fig. 4B; $p<0.001$; for CPC/PLGA 10.3 ± 8.5%, for CPC/liquid 8.5 ± 3.0 and for CPC/surface 51.8 ± 7.1%). The release rate per day from day 1–28 (Fig. 4B; % per day) of CPC/surface compared to CPC/liquid was significantly lower ($p<0.01$, release rate of 1.4 ± 0.3% and 2.1 ± 0.1% per day for CPC/surface and CPC/liquid, respectively). Between CPC/surface and CPC/PLGA ($p=0.47$; for CPC/PLGA 1.8 ± 0.4%) and between CPC/PLGA and CPC/liquid ($p=0.14$) no differences were observed.

After 28 days, a significant lower protein retention for CPC/surface was observed compared to CPC/PLGA and CPC/liquid (Fig. 4B; $p<0.0001$; for CPC/PLGA 39.2 ± 4.2%, for CPC/liquid 36.0 ± 3.2% and for CPC/surface 9.9 ± 1.3%).

3.4.3. Osteoinductive capacity of the different formulations

The structural integrity of the scaffolds was maintained in all experimental groups. A fibrous capsule surrounding CPC/control and CPC/porous, without the presence of inflammatory cells at the interface was observed (data not shown). Ingrowth of soft tissue was observed peripherally in CPC/control and throughout the implants in CPC/porous and no bone formation was observed in the vicinity of these scaffolds. A fibrous capsule surrounding CPC/PLGA, CPC/liquid and CPC/surface, without the presence of inflammatory cells at the interface was observed (data not shown). In 4 out of 5 CPC/surface, a limited amount of bone was formed at the periphery of the scaffold, while no bone formation was observed in the vicinity of CPC/PLGA and CPC/liquid scaffolds (Fig. 5B). Back-scatter SEM micrographs confirmed the observed peripheral bone formation in CPC/surface (Fig. 5C). Quantitative results of ectopic bone formation revealed a total amount of bone in the periphery of CPC/surface of 3.6 ± 3.0 mm^2.

4. Discussion

To enhance the biological performance of CPC biologically active compounds, such as BMP-2, can be introduced. The clinical application of CPC in an injectable form requires an integrated loading of BMP-2 via either PLGA-microparticles or the liquid phase of the cement. In view of this, the current study comparatively evaluated the in vitro and in vivo release profiles as well as the osteoinductive potential of CPC scaffolds in a rat subcutaneous implantation model, in which BMP-2 was (i) loaded onto dense PLGA-microparticles (CPC/PLGA), (ii) added to the liquid phase of the cement (CPC/liquid), or (as a control) (iii) adsorbed onto the surface of preset scaffolds (CPC/surface). It was hypothesized that in view of an injectable CPC, the addition of BMP-2 via incorporated PLGA-microparticles would result in an accelerated BMP-2 release leading to improved osteoinductive properties for CPC/PLGA compared to CPC/liquid. The in vitro and in vivo release assays revealed that the BMP-2 burst release from CPC/surface was significantly increased compared to CPC/PLGA and CPC/liquid. The BMP-2 retention for CPC/surface was significantly lower after 28 days compared to CPC/PLGA and CPC/liquid, despite a significantly increased sustained release rate for CPC/PLGA and CPC/liquid. The ectopic rat model demonstrated that only CPC/surface is capable of inducing ectopic bone formation.

The release profiles of the different scaffold formulations revealed similar patterns consisting of a burst release followed by a sustained release. However, the cumulative release was significantly increased at all time points for surface-loaded BMP-2 compared to that for incorporated BMP-2 (via either PLGA-microparticles or the liquid phase of the CPC). This difference in cumulative release is mainly dependent on the large difference (~30% in vitro, ~40% in vivo) in burst release observed for surface-loaded BMP-2 compared to that for incorporated BMP-2. The difference in burst release is likely to be related to the manufacturing process of the different scaffolds, which results in an evidently distinct protein distribution. Surface loaded BMP-2, was located peripherally and hence in direct contact with the surrounding environment in which BMP-2 could be released fast and freely. In contrast, incorporated BMP-2 was located throughout the CPC and hence any released BMP-2 had to diffuse out of the scaffold. In addition, the protein diffusion within CPC is dependent on the scaffold porosity, for which differences existed regarding the temporal presence of porosity (i.e. directly for CPC/surface and after degradation of PLGA-microparticles for CPC/PLGA and CPC/liquid). Previous studies have demonstrated that the dense acid terminated PLGA-microparticles degrade in vitro between 2 and 6 weeks [12] and are completely degraded in vivo after 4 weeks (current manuscript) at ectopic locations. In vitro degradation of plain CPC (without PLGA microparticles) starts from week 1 [12,22] and is limited, but can be substantially increased via the effect of acidic degradation products of PLGA. The fact that all 3 experimental groups still show a linear sustained release indicates that degradation (of the CPC) is governing release. However, a relationship between release and porosity is not univocally established. Remarkably, similar release kinetics were observed for CPC/PLGA and CPC/liquid, where it was expected that the rapid degradation of PLGA-microparticles would evoke a faster release of adsorbed BMP-2. In view of this, it appears that liberated BMP-2 molecules from the degraded PLGA-microparticles readily adsorb to the ceramic matrix of CPC, after which overall release kinetics show large similarity to scaffolds with BMP-2 loaded via the liquid phase of the cement [23,24].

The in vivo release of BMP-2 in the current study was ~10–20% higher compared to the in vitro release of the different formulations. However, the observed in vitro and in vivo release kinetics of the different scaffolds followed a similar pattern. These findings corroborate earlier observations, in which despite similar release patterns (i.e. a burst release followed by a sustained release) differences regarding the amounts between the in vitro and in vivo release kinetics of BMP-2 from CPC were observed ranging from 50% [24] to 80% [25]. This difference is likely dependent on the availability of proteins within body fluid and the large buffering capacity of the body, which can be responsible for the difference in release amounts, re-adsorption of the protein and BMP-2 clearance from the vicinity of the scaffold [26]. Therefore, Ruhé, Boerman, Russel, Mikos, Spauwen, and Jansen [24] and Li, Bouxsein, Blake, Augusta, Kim, Li, Wozney, and Seeherman [25] suggested to perform the in vitro release experiment in protein-rich buffer solution to simulate more the body fluid and therefore simulating more the in vivo release of the growth factor. However, for the extrapolation of in vitro data to the in vivo situation protein-rich buffer solution alone was not sufficient because the in vitro release profile of BMP-2 loaded CPC performed in a protein-rich-buffer still underestimated the in vivo release profile with ~20% [24]. Therefore, the predictive value of in vitro release patterns implicates an underestimation of the in vivo situation.

In the current study, the in vivo release of BMP-2 from the different CPC scaffolds was analyzed noninvasively with SPECT imaging. With SPECT the pharmacokinetic profile of ^{125}I-labeled proteins could be monitored quantitatively and the (localization of the) ^{125}I-labeled proteins could be visualized in the rats [27,28]. However, tracking the released ^{125}I-BMP-2 molecules could not be visualized due to limitations in the sensitivity. Nevertheless, due to a fixed implant position, concentrated ^{125}I-BMP-2 molecules in the different scaffolds could be visualized and analyzed accurately and reliably.

Although it seems straightforward to assume that the biological activity of BMP-2 upon loading onto the surface of or into the scaffolds might be compromised, earlier reports and side-experiments in the current study provide evidence to prove this assumption wrong. For example, in the current study as well as previously reported [14], the addition of surface-loaded BMP-2 increased the osteoinductive properties of CPC, indicating no effect on the bioactivity of BMP-2 upon surface loading. In addition, several reports showed that the different loading methods to incorporate BMP-2 into CPC used in the current study (i.e. adsorption of BMP-2 to PLGA-microparticles or addition of BMP-2 to the liquid phase of CPC) are capable to evoke either osteoinductive responses [17,18] or enhance osteogenic responses [19]. Further indirect proof for retained biological activity of BMP-2 was obtained via secondary structure analysis of dissolved BMP-2, which revealed no conformational changes of the protein upon dissolution in the liquid phase of cement. Unfortunately, direct evidence for retained biological activity of BMP-2

upon loading into CPC via adsorption to PLGA-microparticles or addition to the liquid phase remains unavailable, since cell culture experiments with CPC scaffolds or releasate are impossible in view of the effects of calcium release from CPC [29,30]. Taken together, the indirect evidence indicates that the lack of an osteoinductive effect of BMP-2 incorporated within CPC is mainly dependent on an insufficient amount of (burst) released BMP-2 rather than to an altered BMP-2 bioactivity.

Previous reports assumed that for clinical applications in a bone environment, a burst release is needed to result in an "above threshold" amount of exogenous BMP-2 to trigger bone regenerative cells to stimulate bone formation [31–33]. However, lack of consensus exists regarding appropriate amounts of BMP-2 [18,34]. In view of that, the BMP-2 loading methods for injectable CPC used in this study appeared unable to induce bone formation ectopically. This observation is likely to be related not only to the release profile as mentioned earlier, but also to the spatial distribution of BMP-2 throughout the entire scaffold (in contrast to condensed availability at the periphery of the scaffold following surface-loading, which showed osteoinductive capacity). Still, BMP-2 loading for CPC via adsorption to PLGA-microparticles or addition to the liquid phase might be a feasible means to accomplish the stimulation of bone regeneration at orthotopic locations. Further, it has to be emphasized that addition of BMP-2 to the liquid phase of CPC is preferred above adsorption to PLGA-microparticles, since the manufacturing process is more straightforward and less labor-intensive.

In conclusion, the present study demonstrated that BMP-2 loading is feasible for injectable CPC via adsorption to PLGA-microparticles or addition to the liquid phase of CPC. These loading methods resulted in a similar release profile over the course of 28 days, despite distinct protein distribution patterns. Compared to CPC-scaffolds with surface-loaded BMP-2, these loading methods showed a similar release profile, except for a significantly decreased burst release. As such, the observed osteoinductive capacity for only CPC-scaffolds with surface-loaded BMP-2 is likely to be related to this difference in burst release. It remains unclear to what extent the differential BMP-2 loading methods for injectable CPC can affect the biological response in a bone environment.

Acknowledgments

The authors gratefully acknowledge the support of the Smart Mix Program of The Netherlands Ministry of Economic Affairs and The Netherlands Ministry of Education, Culture and Science. The authors thank Natasja van Dijk for assistance with the histological preparations and Dennis Löwik and Britta Ramakers for their assistance with the CD analysis. Scanning electron microscopy was performed at the Nijmegen Center for Molecular Life Sciences (NCMLS), The Netherlands.

References

[1] L.C. Chow, Next generation calcium phosphate-based biomaterials, Dent. Mater. J. 28 (2009) 1–10.
[2] LeGeros, Calcium Phosphate in Oral Biology and Medicine, Karger, Basel, 1991.
[3] M.B. Bohner, Physical and chemical aspects of calcium phosphates used in spinal surgery, Eur. Spine J. 10 (2001) S114–S121.
[4] R. LeGeros, Properties of osteoconductive biomaterials: calcium phosphates, Clin. Orthop. Relat. Res. 395 (2002) 81–98.
[5] J. Jansen, E. Ooms, N. Verdonschot, J. Wolke, Injectable calcium phosphate cement for bone repair and implant fixation, Orthop. Clin. North Am. 36 (2005) 89–95.
[6] W. Habraken, L. de Jonge, J. Wolke, L. Yubao, A. Mikos, J. Jansen, Introduction of gelatin microspheres into an injectable calcium phosphate cement, J. Biomed. Mater. Res. A 87A (2008) 643–655.
[7] D.P. Link, J. van den Dolder, W.J.F.M. Jurgens, J.G.C. Wolke, J.A. Jansen, Mechanical evaluation of implanted calcium phosphate cement incorporated with PLGA microparticles, Biomaterials 27 (2006) 4941–4947.
[8] P. Ruhé, E. Hedberg-Dirk, N.T. Padron, P. Spauwen, J. Jansen, A. Mikos, Porous poly(DL-lactic-co-glycolic acid)/calcium phosphate cement composite for reconstruction of bone defects, Tissue Eng. 12 (2006) 789–800.
[9] P. Ruhé, E. Hedberg, N.T. Padron, P. Spauwen, J. Jansen, A. Mikos, Biocompatibility and degradation of poly(DL-lactic-co-glycolic acid)/calcium phosphate cement composites, J. Biomed. Mater. Res. A 74A (2005) 533–544.
[10] W. Habraken, J. Wolke, A. Mikos, J. Jansen, Injectable PLGA microsphere/calcium phosphate cements: physical properties and degradation characteristics, J. Biomater. Sci. Polym. Ed. 17 (2006) 1057–1074.
[11] R. del Real, J. Wolke, M. Vallet-Regí, J. Jansen, A new method to produce macropores in calcium phosphate cements, Biomaterials 23 (2002) 3673–3680.
[12] R.P. Félix Lanao, S.C.G. Leeuwenburgh, J.G.C. Wolke, J.A. Jansen, In vitro degradation rate of apatitic calcium phosphate cement with incorporated PLGA microspheres, Acta Biomater. 7 (2011) 3459–3468.
[13] R.P. Félix Lanao, S.C.G. Leeuwenburgh, J.G.C. Wolke, J.A. Jansen, Bone response to fast-degrading, injectable calcium phosphate cements containing PLGA microparticles, Biomaterials 32 (2011) 8839–8847.
[14] F.C.J. van de Watering, J.J.J.P. van den Beucken, S.P. van der Woning, A. Briest, A. Eek, H. Qureshi, L. Winnubst, O.C. Boerman, J.A. Jansen, Non-glycosylated BMP-2 can induce ectopic bone formation at lower concentrations compared to glycosylated BMP-2, J. Control. Release (2012), http://dx.doi.org/10.1016/j.jconrel.2011.1012.1041.
[15] H.C. Kroese-Deutman, P.Q. Ruhé, P.H.M. Spauwen, J.A. Jansen, Bone inductive properties of rhBMP-2 loaded porous calcium phosphate cement implants inserted at an ectopic site in rabbits, Biomaterials 26 (2005) 1131–1138.
[16] P.Q. Ruhé, H.C. Kroese-Deutman, J.G.C. Wolke, P.H.M. Spauwen, J.A. Jansen, Bone inductive properties of rhBMP-2 loaded porous calcium phosphate cement implants in cranial defects in rabbits, Biomaterials 25 (2004) 2123–2132.
[17] P. Ruhé, O. Boerman, F. Russel, P. Spauwen, A. Mikos, J. Jansen, Controlled release of rhBMP-2 loaded poly(DL-lactic-co-glycolic acid)/calcium phosphate cement composites in vivo, J. Control. Release 106 (2005) 162–171.
[18] E. Bodde, O. Boerman, F. Russel, A. Mikos, P. Spauwen, J. Jansen, The kinetic and biological activity of different loaded rhBMP-2 calcium phosphate cement implants in rats, J. Biomed. Mater. Res. A 87A (2008) 780–791.
[19] E.J. Blom, J. Klein-Nulend, E.H. Burger, M.A.J. Van Waas, L. Yin, Transforming growth factor-β1 incorporated in calcium phosphate cement stimulates osteotransductivity in rat calvarial bone defects, Clin. Oral Implants Res. 12 (2001) 609–616.
[20] P.J. Fraker, J.C. Speck, Protein and cell membrane iodinations with a sparingly soluble chloroamide, 1,3,4,6-tetrachloro-3a,6a-diphenylglycoluril, Biochem. Biophys. Res. Commun. 80 (1978) 849–857.
[21] H. van der Lubbe, C. Klein, K. de Groot, A simple method for preparing thin (10 microM) histological sections of undecalcified plastic embedded bone with implants, Stain Technol. 63 (1988) 171–176.
[22] R.J. Klijn, J.J. van den Beucken, R.P. Félix Lanao, G. Veldhuis, S.C. Leeuwenburgh, J.G. Wolke, G.J. Meijer, J.A. Jansen, Three different strategies to obtain porous calcium phosphate cements: comparison of performance in a rat skull bone augmentation model, Tissue Eng. Part A 18 (2012) 1171–1182.
[23] T.S. Tsapikouni, Y.F. Missirlis, Protein-material interactions: from micro-to-nano scale, Mater. Sci. Eng. B 152 (2008) 2–7.
[24] P. Ruhé, O. Boerman, F. Russel, A. Mikos, P. Spauwen, J. Jansen, In vivo release of rhBMP-2 loaded porous calcium phosphate cement pretreated with albumin, J. Mater. Sci. Mater. Med. 17 (2006) 919–927.
[25] R.H. Li, M.L. Bouxsein, C.A. Blake, D. D'Augusta, H. Kim, X.J. Li, J.M. Wozney, H.J. Seeherman, rhBMP-2 injected in a calcium phosphate paste (α-BSM) accelerates healing in the rabbit ulnar osteotomy model, J. Orthop. Res. 21 (2003) 997–1004.
[26] P. Laffargue, P. Fialdes, P. Frayssinet, M. Rtaimate, H.F. Hildebrand, X. Marchandise, Adsorption and release of insulin-like growth factor-I on porous tricalcium phosphate implant, J. Biomed. Mater. Res. 49 (2000) 415–421.
[27] D.H.R. Kempen, M.J. Yaszemski, A. Heijink, T.E. Hefferan, L.B. Creemers, J. Britson, A. Maran, K.L. Classic, W.J.A. Dhert, L. Lu, Non-invasive monitoring of BMP-2 retention and bone formation in composites for bone tissue engineering using SPECT/CT and scintillation probes, J. Control. Release 134 (2009) 169–176.
[28] D.H.R. Kempen, L. Lu, K.L. Classic, T.E. Hefferan, L.B. Creemers, A. Maran, W.J.A. Dhert, M.J. Yaszemski, Non-invasive screening method for simultaneous evaluation of in vivo growth factor release profiles from multiple ectopic bone tissue engineering implants, J. Control. Release 130 (2008) 15–21.
[29] D.P. Link, J. van den Dolder, J.G.C. Wolke, J.A. Jansen, The cytocompatibility and early osteogenic characteristics of an injectable calcium phosphate cement, Tissue Eng. 13 (2007) 493–500.
[30] U. Hempel, A. Reinstorf, M. Poppe, U. Fischer, M. Gelinsky, W. Pompe, K.W. Wenzel, Proliferation and differentiation of osteoblasts on biocement D modified with collagen type I and citric acid, J. Biomed. Mater. Res. B 71B (2004) 130–143.
[31] H. Seeherman, J.M. Wozney, Delivery of bone morphogenetic proteins for orthopedic tissue regeneration, Cytokine Growth Factor Rev. 16 (2005) 329–345.
[32] J.W.M. Vehof, A.E. de Ruijter, P.H.M. Spauwen, J.A. Jansen, Influence of rhBMP-2 on rat bone marrow stromal cells cultured on titanium fiber mesh, Tissue Eng. 7 (2001) 373–383.
[33] J. van den Dolder, A.J.E. de Ruijter, P.H.M. Spauwen, J.A. Jansen, Observations on the effect of BMP-2 on rat bone marrow cells cultured on titanium substrates of different roughness, Biomaterials 24 (2003) 1853–1860.
[34] R.E. Jung, F.E. Weber, D.S. Thoma, M. Ehrbar, D.L. Cochran, C.H.F. Hämmerle, Bone morphogenetic protein-2 enhances bone formation when delivered by a synthetic matrix containing hydroxyapatite/tricalciumphosphate, Clin. Oral Implants Res. 19 (2008) 188–195.